

DOI: 10.17516/1998-2836-0260

УДК 548.736.372

The Physicochemical Analysis of Bayerite $\text{Al}(\text{OH})_3 \rightarrow \gamma\text{-Al}_2\text{O}_3$ Transformation

Natalya V. Filatova*,

Nadezhda F. Kosenko and Artyom S. Artyushin

*Ivanovo State University of Chemistry and Technology
Ivanovo, Russian Federation*

Received 29.10.2021, received in revised form 07.11.2021, accepted 30.11.2021

Abstract. It was obtained aluminum hydroxide in the form of bayerite by precipitation with ammonia. The precipitation pH was found by the potentiometric titration. Based on the data of thermal, X-ray diffraction and IR-analysis it was identified the sequence of bayerite transitions up to 800 °C. The study of nitrogen adsorption-desorption allowed to determine a specific surface, a volume, and dimensions of pores for boehmite and $\gamma\text{-Al}_2\text{O}_3$ as 135 ± 2 and 238 ± 10 m²/g; 0.38 and 0.51 cm³/g; 1.7 and 3.8 nm, relatively. The value of effective activation energy for boehmite $\rightarrow \gamma\text{-Al}_2\text{O}_3$ transition ((136 ± 5) kJ/mol) was found by means of non-isothermal method (by Avrami equation).

Keywords: boehmite, $\gamma\text{-Al}_2\text{O}_3$, bayerite, thermolysis, dehydration kinetics, Avrami equation, activation energy, thermal analysis, diffractograms.

Acknowledgements. The study was carried out using the resources of the Center for Shared Use of Scientific Equipment of the ISUCT (with the support of the Ministry of Science and Higher Education of Russia, grant No. 075-15-2021-671) The study was carried out using the resources of the Center for Shared Use of Scientific Equipment of the ISUCT (with the support of the Ministry of Science and Higher Education of Russia, grant No. 075-15-2021-671).

Citation: Filatova, N. V., Kosenko, N. F., Artyushin, A. S. The physicochemical analysis of bayerite $\text{Al}(\text{OH})_3 \rightarrow \gamma\text{-Al}_2\text{O}_3$ transformation, J. Sib. Fed. Univ. Chem., 2021, 14(4), 527–538. DOI: 10.17516/1998–2836–0260

Физико-химический анализ перехода байерита $\text{Al}(\text{OH})_3$ в $\gamma\text{-Al}_2\text{O}_3$

Н. В. Филатова, Н. Ф. Косенко, А. С. Артюшин

*Ивановский государственный
химико-технологический университет
Российская Федерация, Иваново*

Аннотация. Получен гидроксид алюминия в виде байерита осаждением аммиаком. рН осаждения определен методом потенциометрического титрования. На основании данных термического, рентгенофазового и ИК-спектрального анализа установлена последовательность превращений байерита в интервале температур до 800 °С. По данным адсорбции-десорбции азота для образующихся бёмита и $\gamma\text{-Al}_2\text{O}_3$ определена удельная поверхность, объем и средний размер пор: 135 ± 2 и 238 ± 10 м²/г; 0,38 и 0,51 см³/г; 1,7 и 3,8 нм соответственно. Неизотермическим методом (по уравнению Аврами) оценена эффективная энергия активации перехода байерит→бёмит: (136 ± 5) кДж/моль.

Ключевые слова: бёмит, $\gamma\text{-Al}_2\text{O}_3$, байерит, термолиз, кинетика разложения, уравнение Аврами, энергия активации, термический анализ, дифрактограммы.

Благодарности. Исследование проведено с использованием ресурсов Центра коллективного пользования научным оборудованием ИГХТУ (при поддержке Минобрнауки России, соглашение № 075-15-2021-671).

Цитирование: Филатова, Н. В. Физико-химический анализ перехода байерита $\text{Al}(\text{OH})_3$ в $\gamma\text{-Al}_2\text{O}_3$ / Н. В. Филатова, Н. Ф. Косенко, А. С. Артюшин // Журн. Сиб. федер. ун-та. Химия, 2021, 14(4). С. 527–538. DOI: 10.17516/1998–2836–0260

Introduction

Alumina is an inorganic material which is widely used in ceramics [1], catalysts and catalysts supports [2], photocatalysts [3], hydrogen production [4], as electronic material [5], and in other fields. Materials on the base of aluminum oxides and hydroxides are among the most studied. In recent years, the increasing attention has been focused on the development of alumina nano-sized powders. They have a high potential as composites [6], as binder in no cement high alumina castable [7], for pollution prevention [8], as biocompatible material for medical composites [9], etc. In the literature, there are many methods of the nano alumina preparation by different methods such as sol-gel [10], combustion [11], hydrothermal [12] and other liquid phase synthetic methods [13]. Currently, the most common route is the thermal decomposition of aluminum hydroxides and oxyhydroxides. Hydroxides are usually obtained by precipitation [14–21]. There were used various precipitating agents, such as NaOH and n-butylamine [15], ammonium acetate [16], ammonium carbonate [17], ammonium bicarbonate [18], soda [19], ammonia [20], sodium carbonate [21].

Gibbsite and bayerite are the most important aluminum trihydroxides $\text{Al}(\text{OH})_3$ [20,22–24]. Among aluminum hydroxides, boehmite, aluminum oxyhydroxide AlOOH , is an accepted precursor because of its heat treatment produces transition aluminas [25]. Boehmite γ - AlOOH is one of two polymorphs of aluminum oxyhydroxide (the other one is diasporite, α - AlOOH). Boehmite can be prepared by a solid-state thermal transformation of gibbsite [26, 27]. Boehmite can be also synthesized from a liquid phase by hydrothermal/solvothermal routes or by sol-gel and precipitation techniques [28]. Experimental conditions such as an aluminum source, the nature of a precipitating agent, pH, temperature, and time of a thermal treatment may have the main influence on the boehmite crystallite size and morphology [29]. γ -Alumina is a kind of extremely important nano sized materials. It is used as a catalyst, can promote the sintering behavior of alumina, etc. [1, 2]. The characterization of transition aluminas formed by the dehydration of boehmite have been extensively studied [25, 27]. It was also under investigation the mechanism and kinetic parameters of the thermal decomposition of gibbsite and bayerite by non-isothermal thermogravimetric analysis [30–32].

In this paper, we tried to describe the bayerite \rightarrow boehmite $\rightarrow \gamma$ - Al_2O_3 thermal decomposition, to give some characteristics of obtained boehmite and γ - Al_2O_3 , and to determine the activation energy of the bayerite dehydration under non-isothermal conditions.

Materials and experiments

Aluminum nitrate nonahydrate $\text{Al}(\text{NO}_3)_3 \cdot 9\text{H}_2\text{O}$, analytically grade, in the form of 0.25 M solution in a distilled water was under stirring. The ammonium hydroxide solution (chemically pure, 6 M) was added to this solution during 1.5 h under constant stirring to pH 9.1–9.3. The precipitate was filtered, washed with distilled water, filtered again, and dried at 100–105 °C to a powder which was ground in a mortar. Dried precursor was heated at a rate of 10 °C/min in air atmosphere up to required temperature in a muffle oven SNOL 1300.

XRD-patterns were obtained using a diffractometer DRON-6 with a copper target ($\lambda=0.1542 \text{ \AA}$, 40 kV, 100 mA). Thermal analysis was performed in a computer-controlled instrument (model TGA/SDTA851°/LF/1600); crucible 700 mkL; air blow 50 mL/min; temperature program up to 1200 °C at various heating rates (2, 3, 5, 10, 15, 20, 30, and 50 °C/min). Infrared spectra of samples were obtained on Avatar 360-FT-IR spectrometer («Nicolet»). The nitrogen adsorption-desorption measurements of calcined samples were performed using adsorption analyzer Sorbi-MS. The specific surface areas were calculated by means of the Brunauer–Emmett–Teller (BET) method and the pore size distribution was obtained according to the Barret–Joyner–Halenda (BJH) method.

Results and discussion

It was done the direct titration of aluminum nitrate solution by ammonia solution to determine the precipitation pH. The equivalence point was fixed by the potentiometry (Fig. 1). The potential jumps (pH) corresponded to pH of the full precipitation beginning and finish, namely, 3.62 and 9.06, respectively. So, it might consider that pH ~9.1 would provide the $\text{Al}(\text{OH})_3$ full precipitation. According to work [22], under precipitation by ammonia $\text{Al}(\text{OH})_3$ was at first separated as a gel which then was crystallized in the bayerite form. It was confirmed by XRD pattern (Fig. 2).

All main peaks corresponded to bayerite $\text{Al}(\text{OH})_3$ (JCPDS No 21–1307). Boehmite- and gibbsite peaks (JCPDS No 21–1307 and 76–1871, relatively) were not considerable. The process of

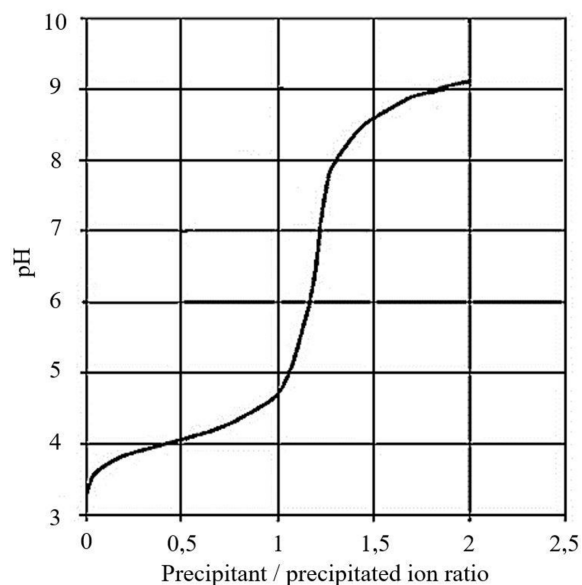


Fig. 1. The titration curve of aluminum nitrate solution by ammonia

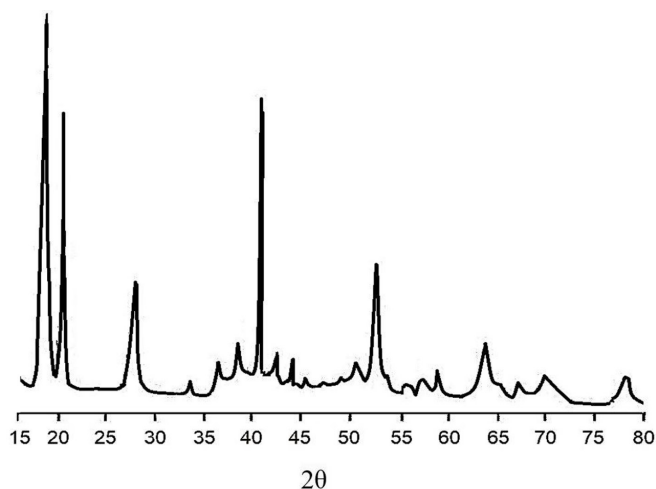


Fig. 2. XRD pattern of a precipitated product. Registered peaks refer to bayerite

its thermal decomposition was complex and run in several stages (Fig. 3). The endotherms at 138 and 203 °C on the DSC curve might refer to the removal of physical and interlaminar water which was in a low quantity [22,27]. The sharp mass loss (~23.5 %) and an intense endothermic peak were observed at ~300 °C. They corresponded to the partial $\text{Al}(\text{OH})_3$ dehydration to monohydrate as boehmite $\gamma\text{-AlOOH}$. Then the removal of expanded water followed to form $\gamma\text{-Al}_2\text{O}_3$ from boehmite (mass loss 14.8 %). All subsequent changes run with no mass loss, so, a gradual heat release in the range of 500–1000 °C and exothermic peaks at 1109 and 1158 °C were attributed to alumina polymorphic transitions up to $\alpha\text{-Al}_2\text{O}_3$ (probably, through δ - and θ -phases). Rough values of the molar water content were calculated as 0.89 (300 °C), 0.19 (450 °C), and 0.07 (600 °C). The

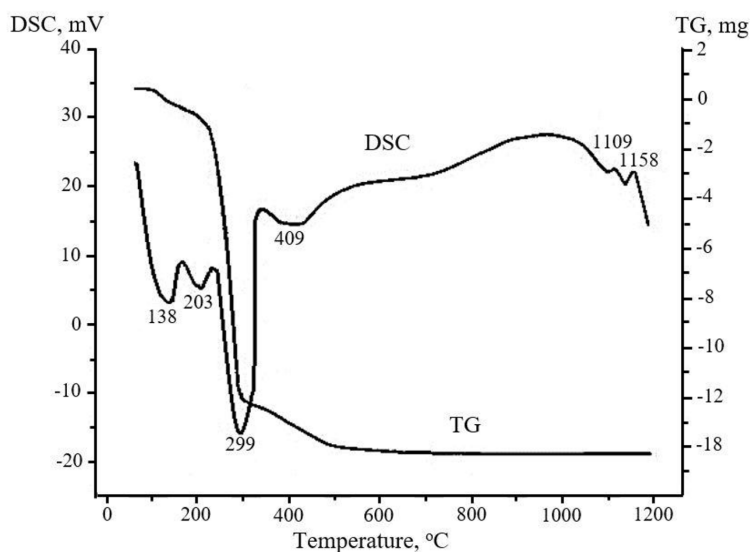


Fig. 3. TG-DSC curves of a dried precipitated product

exotherm appeared at the very end of DTA curve (1158 °C) corresponded to the transformation into α -alumina.

For comparison, DTA curve of the original gibbsite had an intense endotherm around 300–320 °C (gibbsite \rightarrow boehmite) and a second endotherm, less intense, above 500 °C (boehmite \rightarrow γ -alumina) [31]. For the natural boehmite, the dehydroxylation started at 480 °C and was complete by 520 °C [33]. Visible changes of transformations temperatures towards less values might relate to the small particle sizes of bayerite and a fresh boehmite and their high reactivities.

An obtained bayerite was treated at various temperatures for 1 h. XRD patterns indicated the existence of a product up to 250 °C in a XRD amorphous form. At 300 °C clear reflexes were appeared (Fig. 4). According to the JCPDS card No. 21–1307 for γ -AlOOH peaks (2 θ) 14.48, 28.11, 38.25, 45.65, 48.81, 51.44, 55.09, 60.45, 63.88, 64.78, 67.53, 71.73 correspond to hkl positions (020), (120), (031), (131), (051), (220), (151), (080), (231), (002), (171), (251), respectively. So, boehmite represented practically the only phase in the range of 300–400 °C. At 400 °C intensities of boehmite peaks were decreased and their width grew, that might indicate the start of AlOOH decomposition to γ -Al₂O₃ that was confirmed by the data of JCPDS Card No. 29–0063 for this phase: peaks 37.60, 39.49, 45.79, 60.89, 66.76 refer to the (311), (222), (400), (511), (440), respectively. The crystal structure of this polymorph remained up to 800 °C. As seen in Fig. 4, boehmite was transformed completely to γ -alumina. No intermediate compound was found.

The crystallite sizes (D , nm) of crystalline phases were estimated using Debay-Scherrer equation:

$$D = 0.90\lambda/\beta\cos\theta, \quad (1)$$

where λ – X-ray wavelength; β and θ – full-width-at-half-maximum (FWHM) of an observed peak and diffraction angle, respectively.

The calculation of the average crystallite sizes was made using the strongest reflexes (4 for boehmite and 2 for γ -Al₂O₃). They were found as 2.17 (300 °C) and 2.09 nm (400 °C) for boehmite, and 1.69 (500 °C) and 2.08 nm (800 °C) for γ -Al₂O₃.

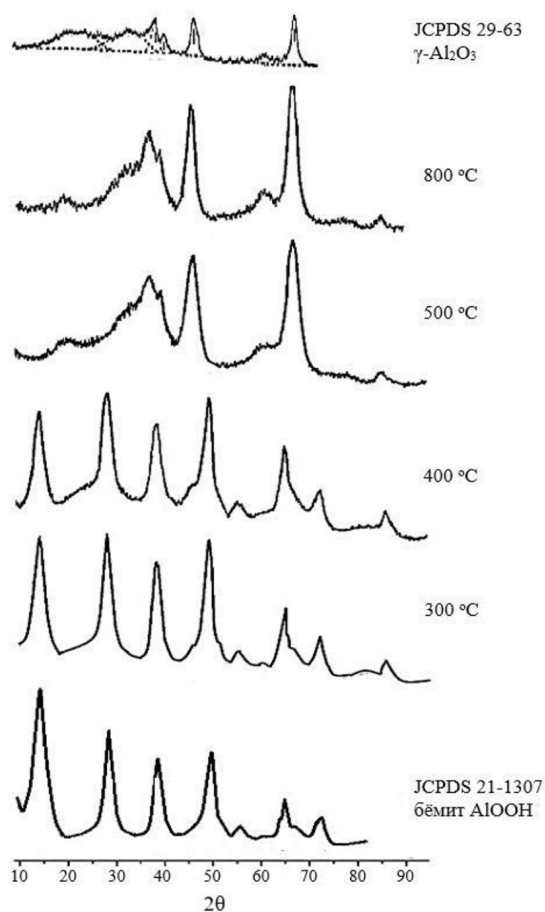


Fig. 4. XRD patterns of a precipitated product

IR-spectra are shown in Fig. 5. The IR spectrum of boehmite had a characteristic $\nu_s(\text{Al})\text{O}-\text{H}$ and $\nu_{\text{as}}(\text{Al})\text{O}-\text{H}$ stretching bands or O–H stretching mode with two maxima at 3380 and $\sim 3050\text{ cm}^{-1}$. The stronger broadening band occurred due to the hydrogen bond between the various hydroxyl groups in boehmite. This was confirmed by the presence of H–O–H bending band at about 1640–1650 cm^{-1} , originating from bending–scissoring vibrations which were typical for water molecules. Boehmite showed strong infrared intensity in the 1050 to 1640 cm^{-1} region [5]. The transmission in the spectra of $\gamma\text{-Al}_2\text{O}_3$ was very weak in this field. Bands presence at $\sim 1160\text{ cm}^{-1}$ (shoulder) and 1050 cm^{-1} corresponded to in-plane bending–scissoring vibration of OH in Al–O–H. The second hydroxyl deformation band at 1050 cm^{-1} related to boehmite [27]. The dehydroxylation of the boehmite followed by the decrease in intensity of the hydroxyl deformation modes. The region of 1000–400 cm^{-1} corresponded to Al–O vibrations for $\gamma\text{-Al}_2\text{O}_3$. The bands at 668, 555, and 461 cm^{-1} were ascribed to the stretching and bending–scissoring vibration modes in octahedral aluminum AlO_6 , while a band at 998 cm^{-1} related to the stretching mode of AlO_4 tetrahedral configuration [5, 27, 33].

Nitrogen adsorption and desorption were measured to investigate the pore characteristics, namely diameter, volume, and size distributions of samples. As shown in Fig. 6, both samples exhibited type IV isotherm with an H2 hysteresis loop according to IUPAC classification, with a capillary condensation

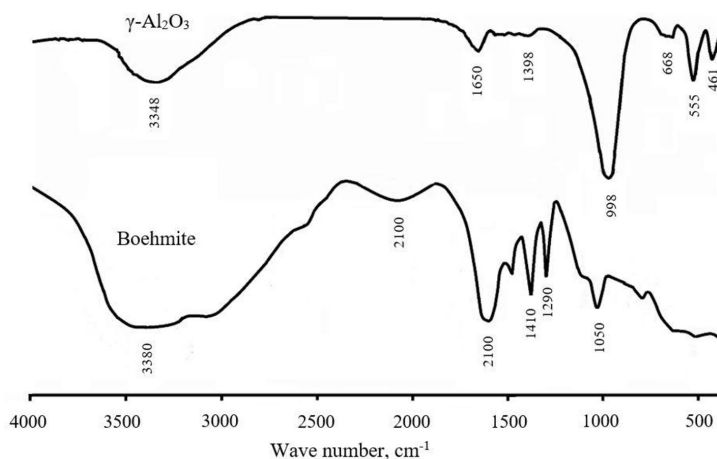


Fig. 5. IR-spectra of a product after heat treatment at 300 °C (boehmite) and 800 °C (γ - Al_2O_3)

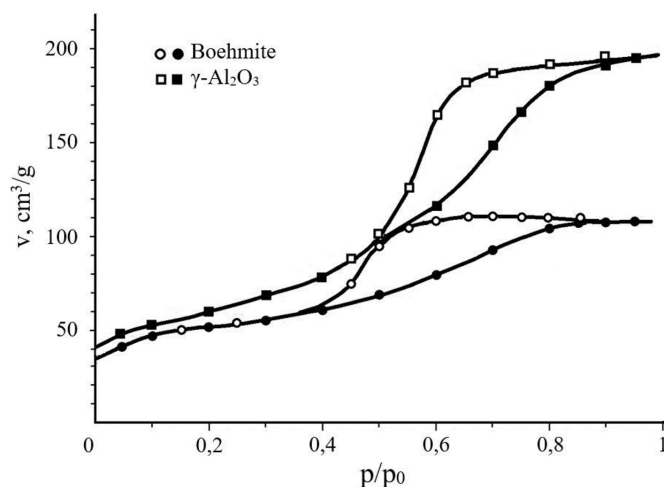


Fig. 6. N_2 adsorption-desorption isotherm plots of boehmite and γ - Al_2O_3 samples

step at $p/p_0 = 0.4\text{--}0.5$. It was the characteristic of a mesoporous material with the presence of cylindrical type pores in both synthesized alumina. Arched initial curve pieces indicated a strong adsorbate-adsorbent interaction. Pore size distributions curves are shown in Fig. 7. Obtained peaks were single with narrow pore size distribution. The pore size distribution plots were uniform with one main peak in the ranges of 2–5 nm. It indicated very homogeneous mesopores by size. The average pore sizes were found as 1.7 and 3.8 nm, respectively.

Specific surface areas, S_{BET} , were 135 ± 2 and 238 ± 10 m^2/g for boehmite and γ - Al_2O_3 . Pore volumes were around 0.38 and 0.51 cm^3/g , respectively.

Thermal analysis techniques were used in the evaluation of kinetic parameters of solid-state reactions in the dehydroxylation process of bayerite powder. $\text{Al}(\text{OH})_3$ decomposition to boehmite was accompanied by the heat absorbance, that is revealed as endoeffect in DTA/DSC curves. Fig. 8 illustrated DSC curves fragments for bayerite \rightarrow boehmite transition.

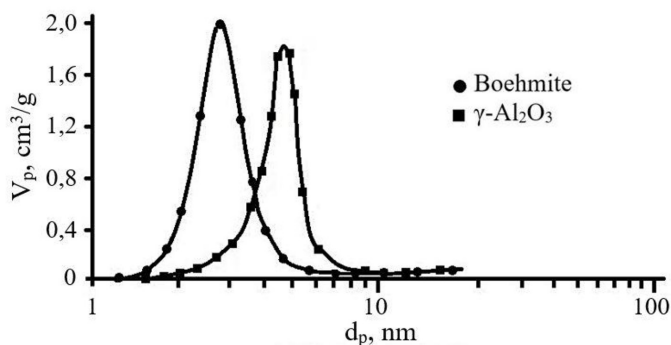


Fig. 7. Pore size distribution for boehmite and γ - Al_2O_3 samples

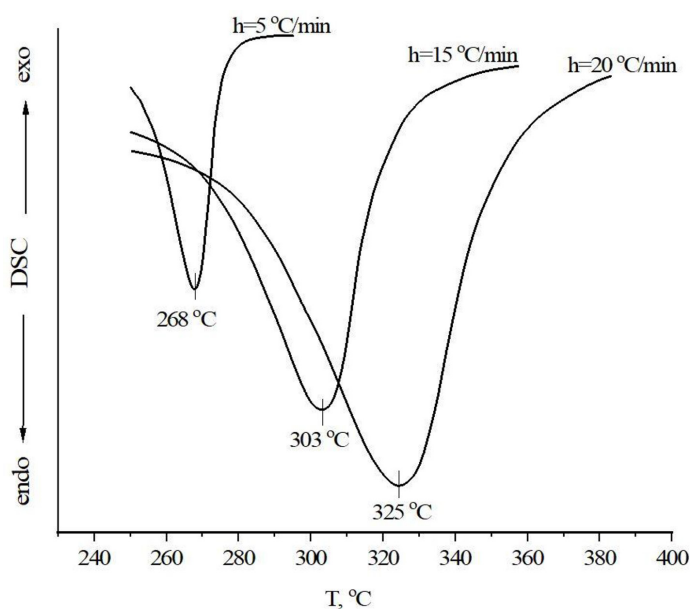


Fig. 8. DSC curve fragments for bayerite \rightarrow boehmite transition at various heating rates of samples

These fragments differed by the heating rate during curves registration and by the extremum temperature. Peak temperatures of each endothermic curve shifted to the higher temperatures with the heating rate increase. It meant that dehydration temperature was not fixed but grew with increasing of heating rate. These data could be used to make a kinetic analysis of boehmite dehydration by Avrami equation:

$$\ln\left(\frac{T_{max}^2}{h}\right) = \frac{E_a}{RT_{max}} + \ln\frac{E_a}{RA'} \quad (2)$$

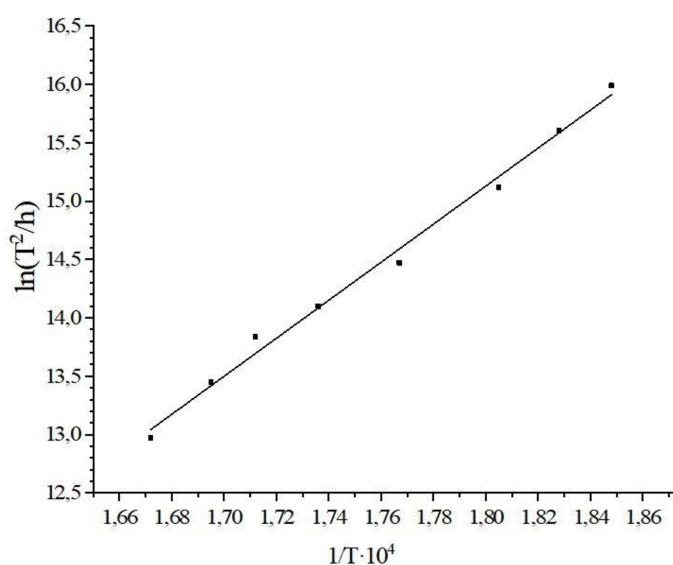
where T_{max} – endothermic peak temperature which related to dehydration reaction; h – heating rate, K/c ; E_a – effective activation energy, J/mol ; R – universal gas constant ($8,314 J/mol\cdot K$); A – pre-exponential factor in Arrhenius equation:

$$k = A \exp(-E_a/RT). \quad (3)$$

The plot of $\ln\left(\frac{T_{max}^2}{h}\right)$ versus $\frac{1}{T_{max}}$ expected to be linear with slope $\text{tg}\alpha$. So, the activation energy could be attained via this expression as $E_a = R \cdot \text{tg}\alpha$. Experimental and calculated data are presented in Table 1. Values of $\text{tg}\alpha$ (16.3 ± 0.6) and coefficient of correlation R^2 (0.975) were determined from slope of the dependence given in Fig. 9.

Table 1. Data for the effective activation energy estimation by Avrami equation

T_{max} , K	541	547	554	566	576	584	590	598
h , K/min	2	3	5	10	15	20	30	50

Fig. 9. The Avrami plot for bayerite \rightarrow boehmite transition

The effective activation energy for the partial bayerite dehydration and boehmite formation was calculated as 136 ± 5 kJ/mol. This magnitude was in accordance with the activation energy value for gibbsite \rightarrow boehmite transition which was estimated by different authors in the range of 155–159 kJ/mol [30], 108.5 kJ/mol [31], 133–142 kJ/mol [32].

Conclusion

Aluminum hydroxide as bayerite was precipitated with ammonia. The process of its thermal decomposition was complex and run in several stages. XRD patterns indicated the existence of a product up to 250 °C in an amorphous form. The boehmite represented practically the only phase in the range of 300–400 °C. At 400 °C AlOOH was decomposed to $\gamma\text{-Al}_2\text{O}_3$. No intermediate compound was found. The specific surface, volumes, and dimensions of pores for boehmite and $\gamma\text{-Al}_2\text{O}_3$ were determined as 135 ± 2 and 238 ± 10 m²/g; 0.38 and 0.51 cm³/g; 1.7 and 3.8 nm, relatively. First, the effective activation energy for bayerite \rightarrow boehmite transition (136 ± 5 kJ/mol) was found by means of

non-isothermal method (by Avrami equation). It was compared with the analogous value for gibbsite → boehmite transition.

References

1. Abyzov A. M. Aluminum Oxide and Alumina Ceramics (review). Part I. Properties of Al_2O_3 and Commercial Production of Dispersed Al_2O_3 . *Refractories and Industrial Ceramics* 2019. Vol. 60(1), P. 24–32.
2. Nishimura S., Ohmatsu S., Ebitani K. Selective synthesis of 3-methyl-2-cyclopentenone via intramolecular al-dol condensation of 2,5-hexanedione with $\gamma\text{-Al}_2\text{O}_3/\text{AlOOH}$ nanocomposite catalyst. *Fuel Processing Technology* 2019. Vol. 196, 106185. <https://doi.org/10.1016/j.fuproc.2019.106185>.
3. Munusamy G., Varadharajan K., Narasimhan S., Thangapandiyam U. G. Investigation of $\gamma\text{-AlOOH}$ and NiWO_4 -coated boehmite micro/nanostructure under UV/visible light photocatalysis. *Research on Chemical Intermediates* 2018. Vol. 44, P. 7815–7834.
4. Kaddissy J. A., Esnouf S., Saffré D., Renault J. P. Efficient hydrogen production from irradiated aluminum hydroxides. *International Journal of Hydrogen Energy* 2019. Vol. 44(7), P. 3737–3743.
5. Fornari R. Single crystals of electronic materials: growth and properties. Woodhead Publishing: Cambridge, UK, 2018. P. 594.
6. Yang Z., Qi C., Zheng X., Zheng J. Synthesis of $\text{Ag}/\gamma\text{-AlOOH}$ nanocomposites and their application for electrochemical sensing. *Journal of Electroanalytical Chemistry* 2015. Vol. 754, P. 138–142.
7. Singh A. K., Sarkar R. High alumina castables: effect of alumina sols and distribution coefficients. *Transactions – Indian Ceramic Society* 2016. Vol. 74(4), P. 225–231.
8. Tao W., Zhong H., Pan X., Wang P., Wang H., Huang L. Removal of fluoride from wastewater solution using Ce-AlOOH with oxalic acid as modification. *Journal of Hazardous Materials* 2020. Vol. 384, 121373. <https://doi.org/10.1016/j.jhazmat.2019.121373>.
9. Rahmati M., Mozafari M. Biocompatibility of alumina-based biomaterials – A review. *J. Cellular Physiology*, 2018, 234 (24), DOI: 10.1002/jcp.27292.
10. Виноградов В. В., Дышина Г. А., Виноградов А. В., Агафонов А. В. Бычий сывороточный альбумин, энтрапированный в матрицу оксида алюминия: золь – гель синтез, свойства, термическая стабильность. *Известия вузов. Серия: Химия и химическая технология* 2012. Т. 55(12), С. 3–12. [Vinogradov V. V., Dyshina G. A., Vinogradov A. V., Agafonov A. V. Bovine Serum albumin centr appedintoan alumina matrix: sol – gelsynthesis, properties, thermalstability. *Chemistry and Chemical Technology* 2012. Vol. 55 (12), P. 3–12. (In Russ.)]
11. Behera P. S., Bhattacharyya S. Thermal decomposition, phase evolution and morphology study of combustion synthesized alumina powder – Influence of precursor pH. *Materials Chemistry and Physics* 2021. Vol. 259, 124030. <https://doi.org/10.1016/j.matchemphys.2020.124030>
12. Li S., He H., Tao Q., Xi Y., Chen A., Ji S., Zhang C., Yang Y., Zhu J. Transformation of boehmite into 2:1 type layered aluminosilicates with different layer charges under hydrothermal conditions. *Applied Clay Science* 2019. Vol. 181, 105207. <https://doi.org/10.1016/j.clay.2019.105207>.
13. Behera P. S., Sarkar R., Bhattacharyya S. Nano alumina: A review of the powder synthesis method. *Interceram – International Ceramic Review* 2016. Vol. 65, P. 10–16. <https://doi.org/10.1007/BF03401148>

14. Romero Toledo R., Ruíz Santoyo V., Moncada Sánchez D., Martínez Rosales M. Effect of aluminum precursor on physicochemical properties of Al_2O_3 by hydrolysis/precipitation method. *Nova Scientia* 2018. Vol. 10(20), P. 83–99. <http://dx.doi.org/10.21640/ns.v10i20.1217>
15. Padilla I., López-Andrés S., López-Delgado A. Effects of different raw materials in the synthesis of boehmite and γ - and α -alumina. *Journal of Chemistry* 2016. Vol. 2–3, P. 1–6. <http://dx.doi.org/10.1155/2016/5353490>
16. Ramili Z., Saleh R. Preparation of ordered mesoporous alumina particles via simple precipitation method. *Journal of Fundamental. Sciences* 2008. Vol. 4, P. 435–443.
17. Ruihong Z., Fen G., Yongqi H., Huanq Z. Self-assembly synthesis of organized mesoporous alumina by precipitation method in aqueous solution. *Microporous Mesoporous Mater* 2006. Vol. 93(1–3), P. 212–216. <http://dx.doi.org/10.1016/j.micromeso.2006.02.024>
18. Parida K.M., Pradhan A. C., Das J., Sahu N. Synthesis and characterization of nano-sized porous γ -alumina by control precipitation method. *Materials Chemistry and Physics* 2009. Vol. 113(1), P. 244–248. <http://dx.doi.org/10.1016/j.matchemphys.2008.07.076>
19. Hochepeid J.-F., Ilioukhina O., Berger M.-H. Effect of the mixing procedure on aluminium (oxide)-hydroxide obtained by precipitation of aluminium nitrate with soda. *Materials Letters* 2003. Vol. 57(19), P. 2817–2822. [http://dx.doi.org/10.1016/S0167-577X\(02\)01381-2](http://dx.doi.org/10.1016/S0167-577X(02)01381-2)
20. Тагандурдыева Н., Нараев В. Н., Постнов А. Ю., Мальцева Н. В. Получение гидроксида алюминия – байерита методом осаждения. *Известия СПбГТИ(ТУ)* 2020. 53(79), С. 17–22. <https://doi.org/10.36807/1998-9849-2020-53-79-17-22>. [Tagandurdyeva N., Naraev V. N., Postnov A. Yu., Maltseva N. V. Preparation of aluminum hydroxide – bayerite by precipitation method. *Izvestia SPbSTI (TU)* 2020. N. 53(79), P. 17–22. (In Russ.)]
21. Potdar H.S., Jun K. W., Bae J. W., Kim S. M., Lee Y. J. Synthesis of nano-sized porous γ -alumina powder via a precipitation/digestion route. *Applied Catalysis A: General* 2007. Vol. 321(2), P. 109–116. <http://dx.doi.org/10.1016/j.apcata.2007.01.055>
22. Du X., Su X., Wang Y., Li J. Thermal decomposition of grinding activated bayerite. *Materials Research Bulletin* 2009. Vol. 44(3), P. 660–665. <http://dx.doi.org/10.1016/j.materresbull.2008.06.031>
23. Malki A., Mekhalif Z., Detriche S., Fonder G., Boumaza A., Djelloul A. Calcination products of gibbsite studied by X-ray diffraction, XPS and solid-state NMR. *Journal of Solid State Chemistry* 2014. Vol. 215, P. 8–15. <http://dx.doi.org/10.1016/j.jssc.2014.03.019>
24. Carstens S., Meyer R., Enke D. Towards Macroporous α - Al_2O_3 – Routes, Possibilities and Limitations. *Materials* 2020. Vol. 13(7), 1778. <http://dx.doi.org/10.3390/ma13071787>
25. Szczésniak B., Choma J., Jaroniec M. Facile mechanochemical synthesis of highly mesoporous γ - Al_2O_3 using boehmite. *Microporous and Mesoporous Materials* 2021. Vol. 312, 110792. <https://doi.org/10.1016/j.micromeso.2020.110792>
26. Wang X., Liu G., Qi T., Huang W., Li X., Zhou Q., Peng Zh. Quantitative relationship between the density and structural unit of alpha alumina prepared from gibbsite and boehmite. *Ceramics International* 2021. Vol. 47(8), P. 14464–14474. <https://doi.org/10.1016/j.ceramint.2021.02.025>
27. Van Gog H. First-principles study of dehydration interfaces between diasporite and corundum, gibbsite and boehmite, and boehmite and γ - Al_2O_3 : Energetic stability, interface charge effects, and dehydration defects. *Applied Surface Science* 2021. Vol. 541, 148501. <https://doi.org/10.1016/j.apsusc.2020.148501>

28. Petrakli F., Arkas M., Tsetsekou A. α -Alumina nanospheres from nano-dispersed boehmite synthesized by a wet chemical route. *Journal of the American Ceramic Society* 2018. Vol. 101, P. 3508–3519. <http://dx.doi.org/10.1111/jace.15487>
29. Toledo R.R., Anaya Esparza L.M., Rosales J.M.M. The role of the aluminum source on the physicochemical properties of γ -AlOOH nanoparticles. *Macedonian Journal of Chemistry and Chemical Engineering* 2020, Vol. 39(1), P. 89–99. <http://dx.doi.org/10.20450/mjccce.2020.1929>
30. Redaoui D., Sahnoune F., Heraiz M., Raghdi A. Mechanism and kinetic parameters of the thermal decomposition of gibbsite $\text{Al}(\text{OH})_3$ by thermogravimetric analysis. *Acta Physica Polonica A* 2017. Vol. 131(3), P. 562–565. <http://dx.doi.org/10.12693/APhysPolA.131.562>
31. Zhu B., Fang B., Li X. Dehydration reactions and kinetic parameters of gibbsite. *Ceramics International* 2010. Vol. 36(8), P. 2493–2498. <http://dx.doi.org/10.1016/j.ceramint.2010.07.007>
32. Perić J., Krstulović R., Vućak M. Investigation of dehydroxylation of gibbsite into boehmite by DSC analysis. *Journal of Thermal Analysis* 1996. Vol. 46, P. 1339–1347. <http://dx.doi.org/10.1007/BF01979247>
33. Frost R.L., Klopogge J. Th., Russell Sh.C., Szetu J. Dehydroxylation of Aluminum (Oxo) hydroxides Using Infrared Emission Spectroscopy. Part II: Boehmite. *Applied Spectroscopy* 1999. Vol. 53 (5), P. 572–582.